Radiation Physics and Chemistry 166 (2020) 108451

Contents lists available at ScienceDirect

Radiation Physics and Chemistry

journal homepage: www.elsevier.com/locate/radphyschem

Characterization of the chemical and structural modifications induced by gamma rays on the MAGIC polymer gel

S. BrahimiMoussa[a], M.El.A. Benamar[a], Z. LounisMokrani[b,*]

[a] Laboratory of Fundamental Physic and Applied, University Saad Dahleb Blida, Algeria
[b] Ionizing Radiation Dosimetry Department, Nuclear Research Center of Algiers, Algeria

A B S T R A C T

Understanding the chemistry of radiation-induced polymerization in polymer gel dosimeters is of great importance in the evaluating of the capability, stability and efficacy of the polymer gel to measuring accurately the three-dimensional dose response.

The aim of this work is to characterize the chemical and structural modifications induced by gamma irradiation in normoxic MAGIC polymer gel under different experimental conditions. These modifications have been investigated using FTIR, HPLC, SEM and UV–Visible techniques. Radical formation, chain growth and crosslinking termination processes were considered from FTIR, HPLC results while the polymerized particle sizes were derived from UV–visible and SEM results for different absorbed doses.

1. Introduction

Modern complex conformal radiotherapy techniques such as Intensity Modulated Radiotherapy (IMRT) and Volumetric Modulated Arc Therapy (VMAT) require the use of powerful three dimensional (3D) treatment planning software as well as rigorous control of delivered dose (Webb, 2001; Schreiner, 2017). An accurate dose measurement tool is needed to be clinically qualified for routinely use to evaluate with high precision the patient delivered dose and enable the direct measurement of 3D dose distribution with high resolution (Webb, 2001; Watanabe and Warmington, 2017).

Polymer gel dosimeter remains one of the most attracting dose measurement tools which present many advantages such its capability to record the complex three-dimensional dose distribution, tissue equivalent material, high spatial resolution and possibility of its preparation with varying sizes and geometries (Baldock, 2006, 2017). Over the last twenty years, intensive investigations have been undertaken in order to develop and qualify polymer gel dosimeters with the aim of a routine clinical use regarding the number of publication and proceedings from various Dosgel and IC3D dose meetings (Audet and Schreiner, 1999; Baldock and DeDeene, 2001; Baldock and De Deene, 2004; Lepage, 2006; Maris and Pappas, 2009; Oldham and Newton, 2010; Thwaites and Baldock, 2013; Bäck and Olsson, 2015). These works have provided a solid account of the historical development of 3D dosimetry systems covering the progress in materials used to accumulate the dose information, the evolution in the science and engineering of the imaging systems required to read the information out, the protocols required for reproducible dosimetry and some examples of clinical use illustrating advantage and limitations of the polymer gel dosimetry (Schreiner, 2017). Hence, in order to improve their clinical applicability, a variety of polymer gel compositions were used coupled with different imaging techniques including Magnetic Resonance Imaging MRI, Optical-Computerized Tomography (Optical-CT), and (X-Ray CT) with different protocols and with a diverse range of experimental conditions including the concentration of monomer (methacrylic acid, acrylamide), gelatin, ascorbic acid, copper sulfate, tetrakis hydroxyl methyl phosphonium, temperature, pH, dose and dose rate (Doran et al., 2001; Fong et al., 2001; De Deene et al., 2002; Venning et al., 2004; Luci et al., 2007; Baldock et al., 2010; Hayashi et al., 2010; Johnston et al., 2012).

Watanabe and Warmington (2017) have recently reported that the main factors in the determination of the dose quantification quality are the accuracy, the precision, the spatial resolution the speed and the cost of the reading system. These authors also attest that the gel polymer dosimeter still limited for a routinely use in clinical applications. A review of recent literature reveals that a wide range of uncertainties has been reported for polymer gel systems which are difficult to minimize without determining their origins (Schreiner, 2015; Watanabe and Warmington, 2017). These uncertainties could be attributed to both intrinsic properties of polymer gel dosimeter and scanning performance of the reading systems (De Deene and Vandecasteele, 2013; Jirasek and Hilts, 2014).

Since the formation of physical gel matrix in 3D gel is the conversion under radiation of monomeric components to polymerized

* Corresponding author.
E-mail addresses: b.sounila@gmail.com (S. BrahimiMoussa), z.mokrani@crna.dz (Z. LounisMokrani).

https://doi.org/10.1016/j.radphyschem.2019.108451
Received 6 August 2018; Received in revised form 7 August 2019; Accepted 12 August 2019
Available online 20 September 2019
0969-806X/

particles, so the quantity of polymer formed for a given dose and the size of the precipitated polymerized particles recorded depend on the polymerization process. The chemistry of radiation induced polymerization reactions is complex and includes many processes such as water decomposition, radical formation, chain growth, cross linking and termination (Jirasek and Hilts, 2009). All these chemical processes could affect at different polymerization stage, the dose response of these systems (generally consisting in water, monomer, gelatin and oxygen scavenger). In fact, the polymerization occurs among the monomers, suspended in the gelatin matrix, causing changes in molecular structure and the mass density which consequently could lead to alteration of chemical, optical and magnetic properties. The tridimensional dose distribution is then abstained through the establishment of calibration relationship between the absorbed dose and the amount of quantitative changes measured by different scanning techniques such as MRI, Optical-CT and X-Ray CT. It has been reported by Watanabe (Watanabe et al., 2005; Watanabe and Kubo, 2011) that the accuracy of the dose measured by such detectors depends on the accuracy of the original signal recorded inside the polymer gel medium and the precision of the calibration equation.

It is important to note that there is lack of information dealing with the characterization of the original signal corresponding to the primary modifications induced by radiation in these polymer gel dosimeters. Some few results concerning the consequence of chemistry on gel dosimetry have been discussed in literature (De Deene et al., 2002; Jirasek and Hilts, 2009). The effects of dose and post irradiation time for analyzing polymerized particle size of PAGAT (Poly Acrylamide Gelatin and Tetrakis hydroxyl phosphonium chloride) using spectrophotometry FTIR and UV–Visible have been reported by Samuel (Samuel et al., 2015). Some results on the evaluation of the polymerized particle size for MAGIC-2 (Methacrylic and Ascorbic acid in Gelatin Initiated by Copper) gel dosimetry for different doses and dose rates have been reported by Heather (Heather and Gore, 2006; Samuel et al., 2015).

The main objective of this work is to provide some information on the chemical and structural modifications induced by gamma radiation at different doses in MAGIC polymer gel. Four (04) complementary physico-chemical techniques have been used for this characterization. Hence, Fourier Transform Infra Red spectrophotometry (FTIR) analysis is used to study the effect of gamma rays on principal chemical bands of the polymer gel for the identification of active chemical species and their implication in the polymerization process. High Performance Liquid Chromatography (HPLC) analysis is used in order to quantify the change affected each compound in MAGIC polymer gel dosimeter as function of gamma irradiated dose and to highlight the role of gelatin in the polymerization process. The UV–Visible spectrophotometry is used to examine the change in optical proprieties and to evaluate the evolution of light scattering particle as function of the gamma dose and finally the Scanning Electron Microscopy (SEM) analysis is used to provide information on the structure and morphology of the polymerized particles and their evolution with the dose.

2. Materials and methods

2.1. Gel preparation

MAGIC polymer gel, in its basic form as introduced by Fong et al. (2001), has been selected for this study. In fact, MAGIC material has been intensively investigated leading to generation of a great number of radiological and physico-chemical data.

The MAGIC gel preparation needs: high-pressure liquid chromatography grade pure water, gelatin ($C_{17}H_{32}N_5O_6$, porcine skin, 250 bloom), ascorbic acid ($C_6H_8O_6$), copper sulfate ($CuSO_4{\cdot}5H_2O$), methacrylic acid (M.A., $C_4H_6O_2$), hydroquinone ($C_6H_6O_2$) (all above from Biochim). MAGIC gel is prepared with the following Fong procedure: for 100 ml of gel, 8% of gelatin is mixed with 80% de-ionized water (Fong et al., 2001). The mixture was heated to 50 °C and strongly stirred with a magnetic bar (300 revolution per minute) until gelatin was completely melted (during approximately 1 h (1 h)). When the emulsion was obtained, hydroquinone ($1.8\ 10^{-2}$ M) was then added in the mixture, still stirred, and the heater was turned off. Ascorbic acid ($2.0\ 10^{-3}$ M) and copper sulfate solutions ($1.8\ 10^{-5}$ M) were added when the mixture was cooled to 37 °C. After 2min, 9% of M.A. was added and the gel mixture was stirred for two more minutes. The gel was then transferred into 10 ml glass tubes, sealed with screw-cap tops and kept in refrigerator at 4 °C during 24 h for gel stabilization. Hence, for all our study the time between gel preparation and gel irradiation is fixed to one day.

2.2. Irradiations

Irradiations have been performed under reference conditions (at normal incidence in a field size of $10 \times 10 cm^2$) at the Secondary Standard Dosimeter Laboratory (Nuclear Research Center of Algiers, CRNA) using cobalt-60 gamma rays (Eldorado78 from Atomic Energy of Canada limited). The gel phantoms have been placed at a distance of 0.55 m from the source and irradiated in the dose range 0–14 Gy with dose rate of 0.012 Gy/s and a relative expanded uncertainty of 5.2% (k = 2). This dose rate has been experimentally determined in term of air kerma, using a PTW ionization chamber model W-32002 #226 (LS-01) associated with a PTW electrometer UNIDOS #20625 calibrated in IAEA laboratory.

2.3. Characterization analysis systems

2.3.1. FTIR measurements

The IR spectra have been recorded using the PerkinElmer spectrometer in Attenuated Total Reflection (ATR) mode in wavelength ranging from 4000 to 650 cm^{-1} and with a resolution of 2 cm^{-1}. The FTIR/ATR spectra have been recorded by depositing directly the gel samples in their natural state without any pre-preparation.

2.3.2. HPLC measurements

The identification of MAGIC gel compounds was performed by High Performance Liquid Chromatography (HPLC) using the HPLC/DAD Agilent 1100 chromatograph. For the analysis purpose, 0.1 g of MAGIC polymer gel were mixed with 1 mL of methanol and the compounds were separated using ZORBAX SB-C18 column (4.6 mm × 150 mm, 5 μm particle size, 80 Å pore size). The mobile phase consisted of 70% water and 30% acetonitril (v/v). The flow rate was fixed at 1 mL.min-1. The detection has been performed at three wavelengths (200, 230 and 254 nm).

2.3.3. UV–visible measurements

A UV–Visible spectrophotometer (Varian Cary 500) with double beam mode was used to measure simultaneously the absorbance of irradiated MAGIC gel and pristine one. Quartz cuvettes (1 cm optical path) were filled with the solution. The pristine gel is used for baseline correction in spectrophotometer analysis. The absorption wavelength was selected in the range from 200 to 500 nm with a step of 2 nm.

2.3.4. SEM measurements

Scanning Electronic Microscope (SEM) of pristine and irradiated MAGIC polymer have been obtained with JOEL SM-6360 LV microscope with a resolution of 50 nm. Before the SEM observation, the MAGIC gel solution has been first transformed to film by drying into an oven at 40 °C, and then crushed into powder in order to be fixed on the microscope sample holders. The observations have been performed in scanning mode at different acceleration voltages (7, 10, 15 and 20 kV). Different magnifications (X130, X1400 and X1700) have been used in order to follow the evolution of the polymerized particle sizes as function of the absorbed doses.

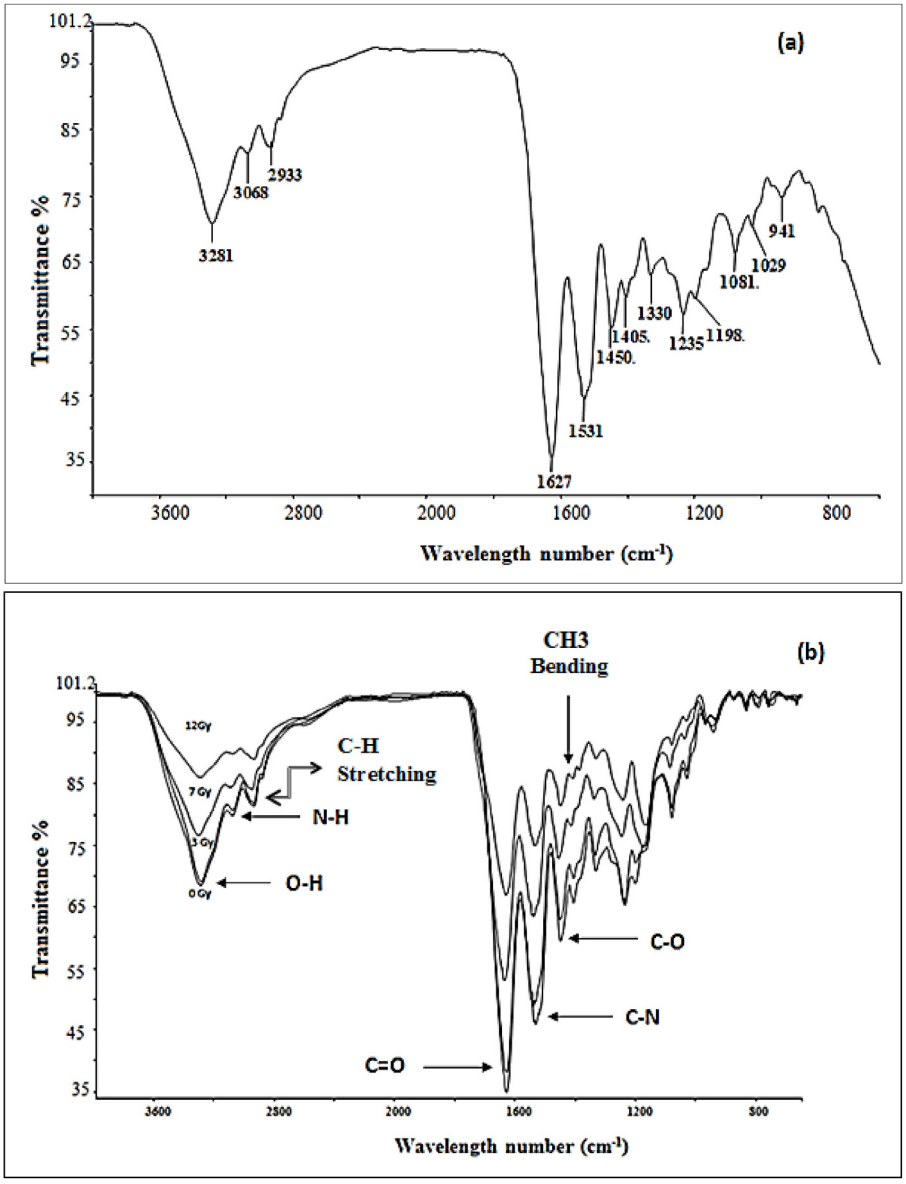

Fig. 1. (a) FTIR Spectrum of MAGIC gel (0 Gy) in the region 600-4000 cm^{-1}. The functional groups characterizing M.A and Gelatin are assigned according to FTIR identification component from Silverstein and Stuart (2004). (b): FTIR Spectra of MAGIC gel irradiated at 0, 3, 7 and 12 Gy and recorded in the region 600-4000 cm^{-1}.

3. Results

3.1. FTIR results

Fig. 1 (a) shows the FTIR spectrum of the MAGIC gel formed from gelatin and methacrylic acid. The major functional groups characterizing M.A. and gelatin have been assigned according to FTIR identification components from Silverstein et al. (2015) and Stuart (2004) and are listed in Table 1. Peaks at approximately 2930 cm^{-1} are identified and associated with symmetrical and asymmetrical CH stretching (CH_2 and CH_3) of the methyl groups. The peak observed at 1531 cm^{-1} is attributed to -C-N-H bending of the peptide bonds of gelatin. However, the small shoulder observed between 1405 and 1330 cm^{-1}, approximately at 1370 cm^{-1} is attributed to a symmetric methyl bending band which is a strong indicator of the presence of the CH_3 methyl groups and also considered as the signature of the CH_3 group attached to carbon atoms.

The C═O carbonyl stretch of the carboxylic acid is expected to appear as an intense band around 1700 cm^{-1}. The apparition of this C═O stretching band around the peak 1627 cm^{-1} is due to the presence of the amide and carboxylic acids of M.A. in the gel. This band has also been observed by Samuel et al. (2015) for PAGAT gel polymer.

In addition, the IR spectrum of the gelatin-M.A. combination for a pristine sample (0Gy) (Fig. 1(a)) shows three characteristic absorption

Table 1
The IR absorption band assignments of the main functional group in MAGIC gel.

Frequency (cm^{-1})	Functional group
3400-3200 (3281)	O–H Stretching band (peptide band)
3068	N–H Stretching
3000-2800 (2933)	C–H Stretching band (CH_2– CH_3)
1660-1600 (1627)	C = O stretching band with band strength intermediare between C═O and C–O in COO^- anion
1565-1500 (1531)	C–N–H Secondary amid N–H bending C–N stretching
1405	C = O Symmetric stretching amide
1370–1380	C–H_3 symmetric bending band
1330 and 1450	C–O Stretching and bending

bands at 1627, 1450 and 1330 cm^{-1}, attesting of the chemical grafting of M.A. on gelatin. These peaks are attributed to the carbonyl stretching of the acid groups and to the symmetric and asymmetric stretching modes of the carboxylate anions (COO^-) respectively. Furthermore, the O–H stretching band appeared in the range of 3200–3500 cm^{-1} is attributed to the combination of the carboxylate and alcoholic absorption.

The effect of irradiation on the chemical structure of the gel can be illustrated by Fig. 1 (b). It represents the MAGIC gel spectra recorded for gel samples irradiated at different doses of 0, 3, 7 and 12Gy. The difference between the pristine (0Gy) and irradiated gel (3, 7, and 12Gy) can be highlighted by the increase of CH_3 methyl group observed as weak peak between 1405 and 1330 cm^{-1}, approximately at 1370 cm^{-1}. The evolution of this band with the dose is a good indicator of the evolution of the polymerization process and the increase of the polymer chain length.

Furthermore, the process of polymerization of M.A. in the MAGIC gel as a function of the absorbed dose can be also followed by comparison of the peak intensities at 1627 and 1450 cm^{-1}. Indeed, from Fig. 1(b), one can note that the intensity of these peaks increases with the dose. This can be attributed to an increase in the contribution of the carbonyl group of the carboxylic acid. The intensity of the band at 3281 cm^{-1} exhibits the same behavior with the dose. Finally, the polymerization process under gamma irradiation is also highlighted by the increase in the intensity of the COO- and OH groups.

3.2. HPLC results

Chromatograms of gelatin solution, gelatin and hydroquinone mixture solution, M.A. monomer solution and the gelatin, M.A. monomer and hydroquinone mixture solution are illustrated in Fig. 2 (a), (b), (c) and (d) respectively. Table 2 shows the main retention time peaks and their corresponding absorbance area and their contribution to the total area (%). It is clear from these data that for the pure solution, the main gelatin peak appears at 1.11min (81%) and M.A. monomer peak at 2.03min (92%). For gelatin with hydroquinone solution, two peaks are observed at 1.8min (68%) and 1.11min (21%). However, for gelatin, M.A. monomer and hydroquinone mixture solution, one can note that the gelatin peak (1.11min) disappears, the M.A. peak shifts to 2.21min (32%) with the presence of the peak at 1.83 min (35%) and a new other peak at 2.46min (32%). This last peak is attributed to M.A. molecules grafted onto gelatin. This is supported by the FTIR results which shows that M.A. molecules (negatively charged) are grafted onto gelatin (positively charged molecules) by chemical bonding. Finally, it is important to note the roughly same contribution of these MAGIC gel compounds to the total absorbance (35, 32, 32%) for 1.8, 2.21 and 2.46 min respectively.

Table 2
Retention times and absorbance area (Absorbance unit, m.AU) recorded at the same wavelength (230 nm) for the main MAGIC compounds (gelatin, M.A. monomer, hydroquinone and gelatin solution, and mixture of hydroquinone, M.A. and gelatin solution).

Main peaks	Tr (min)	Absorbance (m.AU)	Contribution to total area (%)
Gelatin	1.11	947	80.97
M.A	2.03	236	91.93
Hydroquinone/Gelatin	1.12	753	21.24
	1.80	2417	68.23
Hydroquinone/Gelatin/ M.A.	1.83	6414	34.77
	2.21	5980	32.42
	2.46	5930	32.14

Fig. 3 (a), (b), (c) and (d) present HPLC chromatograms of irradiated MAGIC gel at gamma dose of 0, 3, 7, and 10 Gy respectively. The effect of gamma irradiation is examined by following the progress of the three peaks 1.77, 2.25 and 2.46min in terms of their absorbance area and their contribution to the total absorbance. The evolution of HPLC data of these peaks with absorbed dose is summarized in Table 3. For pristine MAGIC, data reveals that more than 49% of gel composition consists in M.A. molecules grafted onto gelatin (2.46min) and 21% free

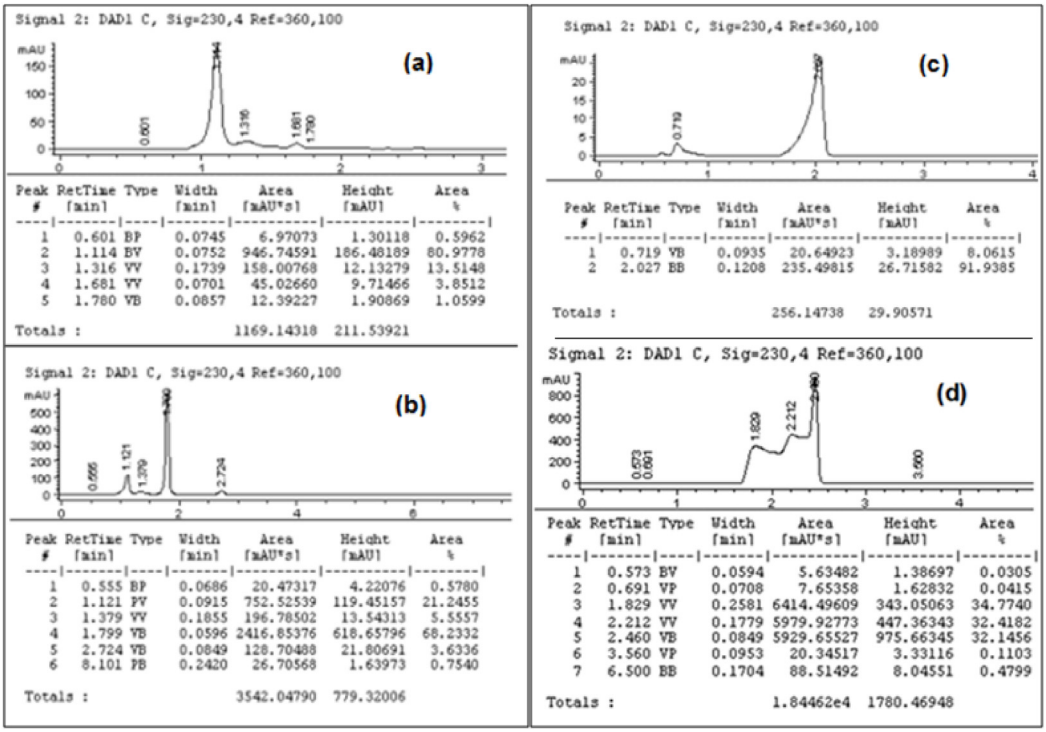

Fig. 2. (a) HPLC chromatograms of gelatin solution (a); hydroquinone and gelatin mixture solution (b); M.A. monomer (c) and hydroquinone, gelatin and M.A. monomer mixture solution (d). These chromatograms are recorded at the same wavelength (230 nm) with injection volume of 5 µL for (a) and (b), 3 µL for (c) and 0.5 µL for (d).

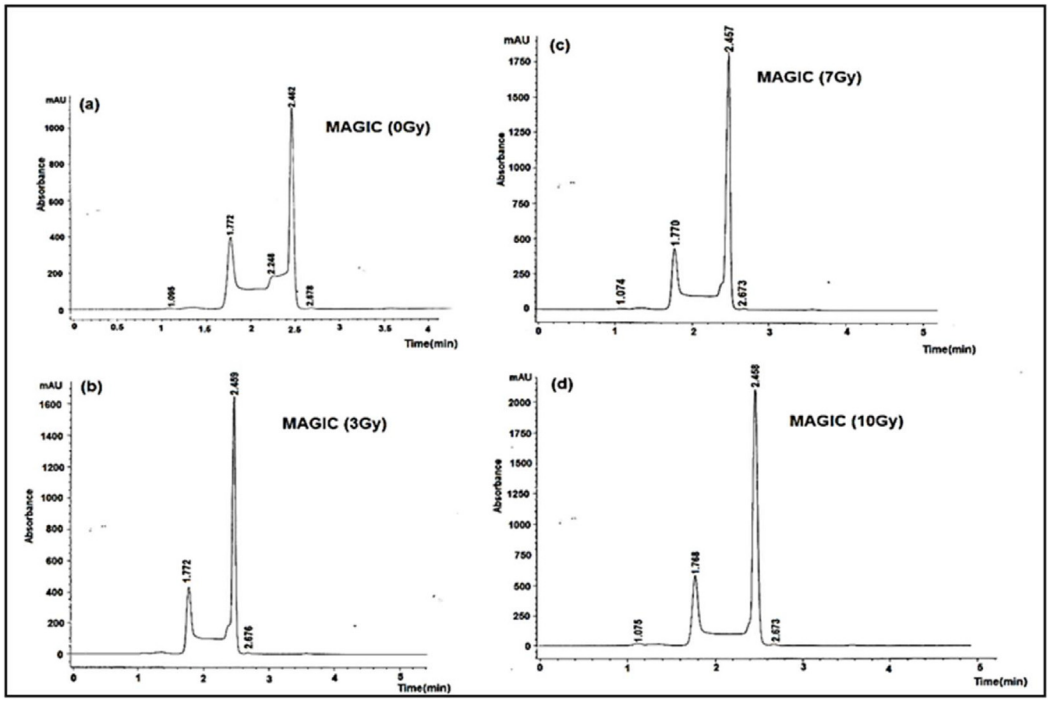

Fig. 3. HPLC chromatograms of MAGIC gel, recorded at 230 nm with the same injection volume of 5 µL, highlighting the effect of gamma dose: 0Gy (a); 3Gy (b); 7Gy (c) and 10Gy (d).

Table 3
Effect of gamma irradiation on the HPLC data of the main MAGIC compounds, obtained at the wavelength of 230 nm with the same injection volume of 5 µL, and evolution of the grafted M.A. and P.M.A. fraction as function of absorbed dose.

Dose (Gy)	Tr (min)	Absorbance (m.AU)	Contribution to total area (%)	Grafted M.A. Fraction (%)	Polymerized Fraction by gamma dose (%)
0	1.77	2957	28.27	/	/
	2.25	2250	21.51	/	/
	2.46	5210	49.81	55.65	0
3	1.77	4602	39.70	/	/
	2.46	6929	59.78	74.02	18
7	1.77	4494	36.60	/	/
	2.46	7721	62.88	82.48	27
10	1.77	5104	35.10	/	/
	2.46	9361	64.38	100	44

M.A. An increase of the contribution of the M.A. grafted fraction from 32 to 49% with a diminution of the contribution of free M.A. monomers from 32 to 21% is observed. This is probably due to MAGIC gel preparation specially the heating and stirring which enhances the M.A. grafting onto gelatin by chemical bonding.

At the dose of 3Gy, an extinction of the M.A. peak is observed with an increase in the fraction of grafted M.A onto gelatin which becomes 60% with proportion of 49% chemically and 11% by conversion of free monomer M.A. molecules to polymethacrylic acid (P.M.A) by irradiation. An equal proportion (about 10%) has been converted to the peak (1.77 min) which shows an enhancement in its contribution (from 28 to 40%). This result confirms the presence of other competitive chemical process for M.A. monomers than polymerization. At higher doses, an increase in the contribution of the peak (2.46min) to about 62% and 64% is observed with a decrease in the contribution of the peak (1.77min) to 37% and 35% for 7 and 10 Gy respectively. It is important to note that the polymerization process continue even in absence of free M.A. monomers in the MAGIC solution and this can only be achieved by consuming the already converted M.A. molecules by a competitive chemical process.

It is important to point out the variation of the contribution of these peaks to total response from (35, 32, 32%) to (35, 0, 64%) at 10 Gy for the peaks 1.8, 2.2 and 2.4 min respectively. This result confirms that all M.A. molecules have been polymerized and grafted onto gelatin.

A quantitative analysis of the data corresponding to the evolution of the peak (2.46min) with absorbed dose is presented in the two last columns of Table 3. One can note that for pristine MAGIC (0Gy), more than 57% of gel composition consists in M.A. molecules grafted onto gelatin by chemical bonding. At the dose of 3Gy, the M.A grafted fraction in gel MAGIC becomes 74% with proportion of 55% chemically and 18% by conversion of free monomer M.A. molecules to polymethacrylic acid (P.M.A) by polymerization process due gamma dose. With the increase of the dose to 7Gy, the conversion fraction due to irradiation attains 27% corresponding to a total grafting fraction of about 82%. Finally, for MAGIC gel irradiated at 10Gy, we observe that all M.A. molecules are bounded in the gel matrix structure leading to a total consummation of M.A. monomers and their conversion to P.M.A. by radiation polymerization process.

Hence, it becomes important to clarify the role of gelatin in this polymerization process. For this purpose, gelatin has been first dissolute in water at 40 °C. This dissolution leads to a mixture of different fraction (polypeptide chain derived from amino acid groups) and then irradiated at absorbed dose of 3 and 7 Gy. Chromatograms presented in Fig. 4 (a, b, c) are obtained from pristine gelatin solution (a) and irradiated ones at different doses (3Gy (b) and 7Gy (c)).

The HPLC chromatogram of pristine sample, Fig. 4(a), reveals five peaks. The retention times and absorbance of gelatin compounds are also summarized in Table 4. The peak of 1.11 min is identified as the main peak of gelatin.

Analysis of HPLC data from Table 4 shows important changes in absorbance intensities between the pristine sample and the irradiated samples at 3Gy. However, no significant changes were observed between the gelatin samples irradiated at 3 and 7Gy. These results suggest that gelatin chemically contribute to the modification of the properties of the MAGIC solution at low doses where it is more sensitive to gamma

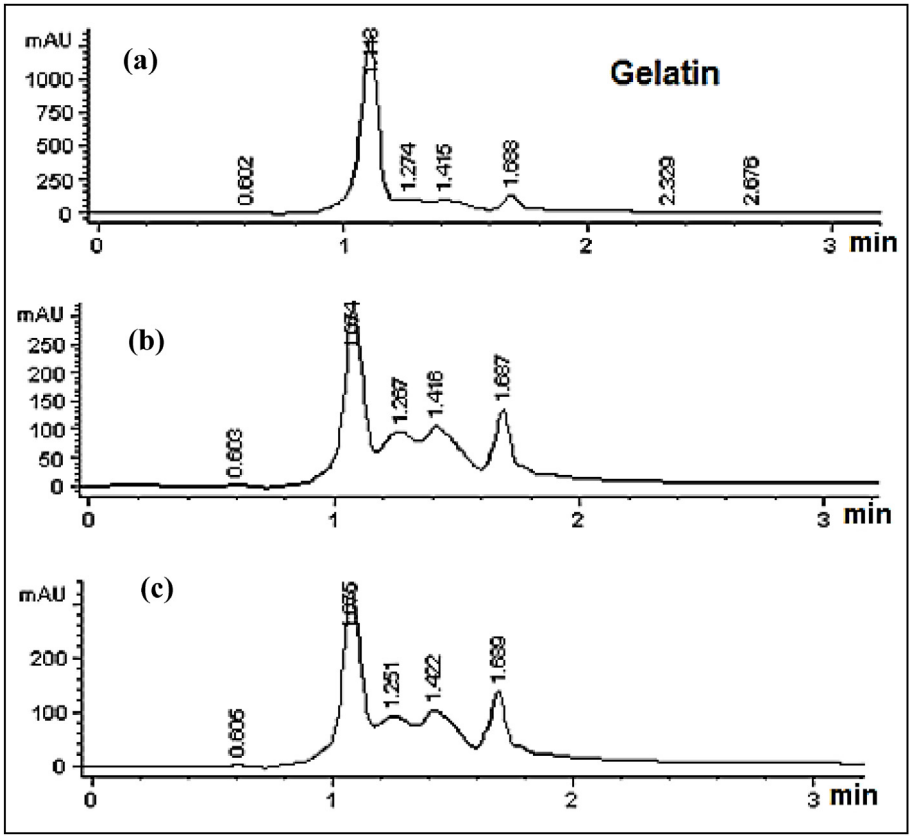

Fig. 4. Identification of the main retention time peaks of gelatin solution. HPLC chromatograms have been recorded at 200 nm with injection volume of 5 μL for irradiated gelatin solution at different doses: 0Gy (a); 3Gy (b) and 7Gy (c).

Table 4
HPLC absorbance area of mean retention time obtained at wavelength 200 nm of the compounds for gelatin at different absorbed doses.

Tr (min)	1.11	1.27	1.42	1.69	2.33
0 (Gy)	7197	749	972	1120	118.8
3 (Gy)	1919	850	1124	1095	0
7 (Gy)	2130	846	1138	1249	0

irradiation. This result is supported by the evolution of the peak 1.77 in MAGIC solution showing an augmentation in its contribution (from 28 to 40%) between 0 and 3 Gy and than return to its initial contribution (35%) at higher doses.

3.3. SEM results

The Fig. 5 (a) and (b) show the SEM photographs of the MAGIC gel irradiated at 10Gy using two observation magnifications (X40 and X130) respectively. These pictures reveal white particles with different sizes (up to 100 μm) and shape embedded in gelatin macromolecules and delimiting the dense region produced by the polymerization of MAGIC gel (PMA) by gamma irradiation. These photographs confirm the role of gelatin to spatially fix the polymerized particles by preventing their diffusion into the MAGIC solution and conferring the 3D propriety of MAGIC dosimeter.

The SEM photographs of the surface of the MAGIC polymer gel for pristine and irradiated samples at different doses (0, 5, 10, 12Gy) are shown in Fig. 6 (a, b, c and d) respectively. Fig. 6(a) for the pristine sample exhibits a smooth, uniform and homogeneous surface. The photographs presented in Fig. 6 (b, c and d) indicate clearly a change in the surface of the MAGIC gel after irradiation where a porous structure is observed. An estimation of these pore diameters from Fig. 6 (b) gives a value of about 294 nm. In addition, from samples irradiated at a dose of 5Gy, it can be seen the formation of few small whitish particles uniformly distributed over the entire surface of the observed field. The increase in the absorbed dose to 10Gy (Fig. 6 (c)) reveals long branches even perpendicular to each other formed by polymerized particles of different shapes and sizes and juxtaposed linearly. The increase of the dose to 12Gy, exhibits a new shape of the polymerized particles with more sophisticated and condensed where it can be noted the presence of nodes and loops (see Fig. 6 (d)), probably formed by dissociation and rearrangement of long branches. These configurations of condensed and knotted polymerized particles illustrate well the three-dimensional structure of the irradiated polymer gel as predicted by Fontanille and Gnanou (2013).

3.4. UV–visible results

The UV–Visible absorption of MAGIC polymer gel curves, as function of wavelength, are presented in Fig. 7 for different doses. These curves show a shift of the maximum absorption edge (λ_{max}) towards the higher wavelength (from 320 to 360 nm) with an increase in the intensity of the main peak with the dose accompanying by a progressive change of the sample color from transparent to opaque.

The dose responses presented in Fig. 8 have been established at two wavelength of 450 and 400 nm and for the maximum absorbance peak intensities. Linear and second polynomial relationship are tested to determine the calibration curves. The quadratic relation seems to be the most appropriate and leads to accurate results. Hence, the precision achieved in the evaluation of the dose using quadratic relationship for different wavelengths is found less than 5% at 3Gy and less than 2% at 7 Gy. It is important to note that the difference reach 65% at 3Gy and 50% at 7Gy when a linear calibration relationship is used. However, no significant difference has been observed between linear and quadratic

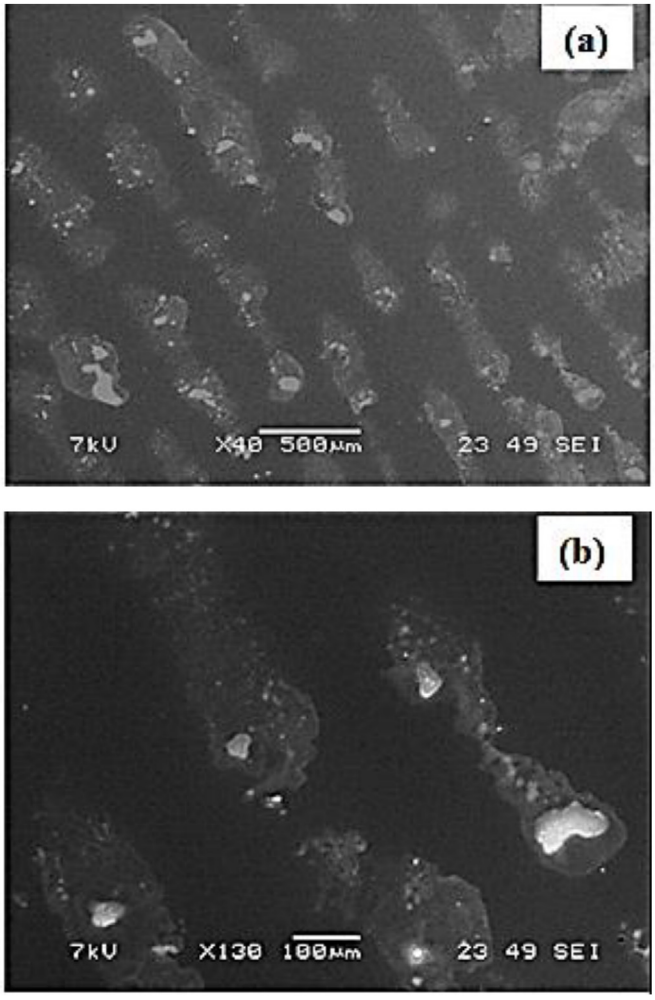

Fig. 5. SEM pictures of the polymerized particles in MAGIC gel irradiated at 10Gy embedded in gelatin and observed with magnification of X40 (a) and X130 (b).

relationship of the calibration curve between the gamma dose and the maximum intensity of UV–visible absorbance which represents the maximum amount of changes induced by absorbed dose in the investigated dose range (0–14Gy). These changes represent to the primary radiation response signal due to the structural and chemical modifications caused by several factors such as the increase of the $-COO^-$ ionized molecules and to the creation of free radicals, scission of polymer chain, unsaturation and cross-linking produced by gamma radiation inducing a decrease in the energy gap of irradiated sample (Siddhartha et al., 2012; Abdel-Fattah et al., 2002).

Furthermore, the evolution of the light scattering particles as a function of the dose is an important parameter affecting the dose response. The size of these polymerized particles has been derived from the UV results using the relation between λ_{max} (nm) and Mie-Debye efficiency factor as reported by Heather and Gore (2006):

$$D = (Ka)\lambda_{max}/n\pi \quad (1)$$

where:"D" (nm) is the diameter of the particle, “Ka” is the Debye efficiency factor (Mie) which is found to be 4.34 (Wickramasinghe, 1973) and “n” is the refraction index which is equal to 1.5 (Heather and Gore, 2006). The particle sizes calculated using equation (1) are reported in Table 5 and also presented in Fig. 9.

The evolution of the diameter of scattering particles as function of the irradiated dose exhibits a quadratic response in the investigated doses range (from 0 to 14Gy). The evolution of the diameter D can be expressed by the following relation:

$$D\ (nm) = 0.37x^2 - 2.45\ x + 293.17 \quad (2)$$

It can be pointed that the calculated pore (particle) diameter (292 nm) of the MAGIC polymer gel for 5Gy is close to that determined from SEM results (294 nm, Fig. 6 (b)).

Finally, the UV results confirm the linearity of the maximum intensity of primary response signal with the dose but the evolution of the diameters of the scattered particles show a quadratic response. However, this primary signal cannot be directly used to evaluate the 3D dose distribution as required for radiotherapy applications and some scanning reading systems are generally used to convert the raw signal into a 3D dose distribution. For the scanning systems which are based on the attenuation principle of light (optical CT reading technique) or X-rays (X-ray CT reading), our results support the assumption of Watanabe and Warmington (2017) which state that the linear equation for calibration is not the most common response characteristics of 3D dosimeters which could be better represented by a second order polynomial equation.

4. Discussion

The FTIR analysis has pointed up the effect of gamma rays on principal chemical bonds of the polymer gel and the identification of some active chemical species such hydroxyl, carboxylate and amine groups (O–H, COO^-, -C-N-H). The gelatin role has also been highlighted in the polymerization process where it has been suggested the chemical grafting of M.A. onto gelatin. In fact, the presence of the carboxylate anions (COO^-) could attest of A.M. onto gelatin grafting in aqueous solution.

Furthermore, the gelatin geometry has been determined using DFT (Density functional theory) with B3LYP functional [Frisch et al., 2009]. Many conformation are proposed but by applying Mulliken's analysis [Frisch et al., 2009], it can be concluded that the most negatively charged atoms in gelatin structure are the nitrogen N94 atoms with a charge of −0.84243. Hence the N94 atoms represent the preferential sites of an electrophilic attack. According to this finding, the grafting of A.M. on gelatin should give the amid group (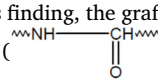), as shown in Fig. 10 (a).

HPLC analysis has permitted to follow the evolution the polymerization of M.A. to PMA by following the grafted fraction in MAGIC polymer gel dosimeter as function of absorbed dose. Fig. 10(b) shows the proposed reaction governing this polymerization and the grafting of P.M.A polymer onto gelatin. From both FTIR and HPLC results, it can be proposed that gelatin is an indispensable component in the polymerization process especially at low doses. In fact, the radicals are first created by the radiolysis of water (H_2O + Radiation → H_2, H_2O_2, e^-_{aq}, $H^{\cdot}$,$OH^{\cdot}$). Since water is acting as an intermediary in inter-chain and intra-chain hydrogen bonding in gelatin solution (RamachandraxG and Chandrasekharan, 1968; Wüstneck et al., 1988), these radicals react in the same time with gelatin and M.A. and cause the initiation of the polymerization of M.A. particles as illustrated in the mechanism proposed in Fig. 11. Hence, the polymerization might be initiated by hydroxyl radical which reacts in the same time with monomer M.A. and gelatin leading to the formation of gelatin and M.A. radicals. The chain could then growing via propagation and chain-transfer reactions which continue to grow until total consummation of M.A. monomers; the termination reactions show a reaction between polymeric radicals and primary radicals and between gelatin radical with monomer radical as proposed by (Jirasek and Hilts, 2009). Furthermore, the formation of the gelatin radical could accelerate the polymerization process at the beginning but by increasing the dose, the crosslinking between different polypeptide gelatin chains leads to the creation of an intense three-dimensional macromolecular network (Carvalho and Grosso, 2008), which explains the gel resistance to gamma radiation since no

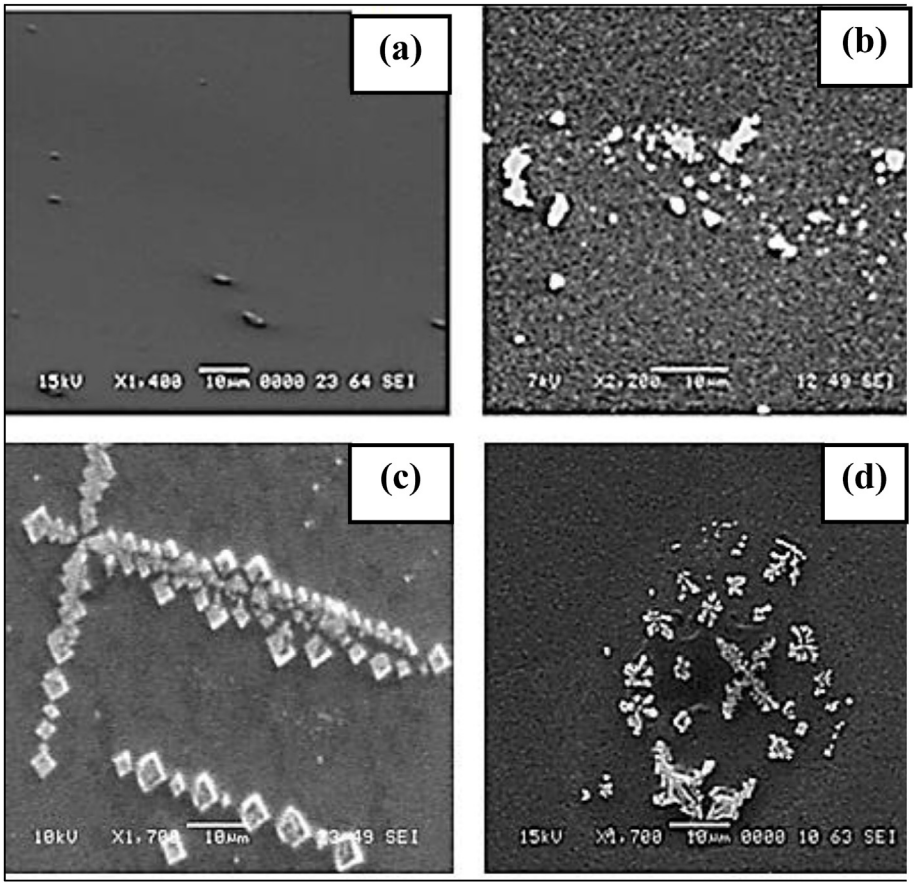

Fig. 6. SEM pictures of the MAGIC gel illustrating the effect of gamma dose (5, 10 and 12 Gy).

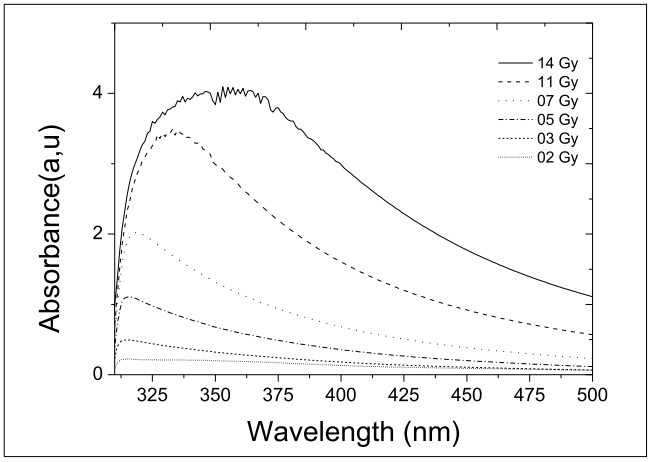

Fig. 7. Absorbance of polymer gel at different doses highlighting the shift of the maximum absorption edge (λ_{max}) towards the higher wavelength (from 320 to 360 nm).

significant effect has been observed beyond 3 Gy. It is important to report here that De Deene have affirmed that the methacrylic acid monomer polymerizes into PMA in the presence of gelatin and does not need to add any crosslinkers because linear polymethacrylic acid polymer precipitates from solution when it is produced in the presence of gelatin (De Deene et al., 2006). This is confirmed by the precipitation of P.M.A. and its fixation in gelatin matrix as shown in Fig. 10(b) and illustrated by Fig. 11. These results are in good agreement with those reported by Hayashi et al. (2010) and confirm that the gelatin role is important at the beginning for the polymerization process where it could act as a trigger and also at high doses where a high dense crosslinked three dimensional network could be created which help the fixation of P.M.A. in the gelatin matrix and prevent their diffusion into the MAGIC solution.

The spectrophotometry UV–Visible and SEM analysis have provided the primary information on changes induced by gamma radiation using light (UV–Visible) and electron (SEM) scattering beams. SEM observations have indicated that the polymerized particles are embedded in macromolecules gelatin and spatially fixed confirming the role of gelatin and the capability of this dosimeter to record 3D dose in continuous medium. In addition, it has been shown that the polymerized particles vary with the dose and present different structures with shapes and sizes far from uniform. This is probably due to competition between the polymerization, the cross linking, dissociation and rearrangement processes which occurred with different MAGIC compounds with the increase of the absorbed dose. The size of the polymerized particles of (288–333 nm) in gamma irradiated MAGIC gel are found in good agreement with those obtained by Heather and Gore (2006) using MAGIC 2 gel (270–334 nm).

Furthermore, the UV–Visible results have shown that the accuracy of the dose measured by a MAGIC polymer gel depends on the calibration equation used in order to convert the raw signal data to the absorbed dose. The use of appropriate calibration curve was essential in performing the “absolute” calibration in this case. Since the polymerized particles which are at the origin of scattered signal for UV–visible reading system presents a quadratic evolution as function of the absorbed dose, a linear calibration would result in highly increased errors and is therefore not recommended for this system. If we want to improve the accuracy of dose measurement, it is recommended to use a second order polynomial calibration relationship and not linear, especially for reading systems based on the attenuation principle such as

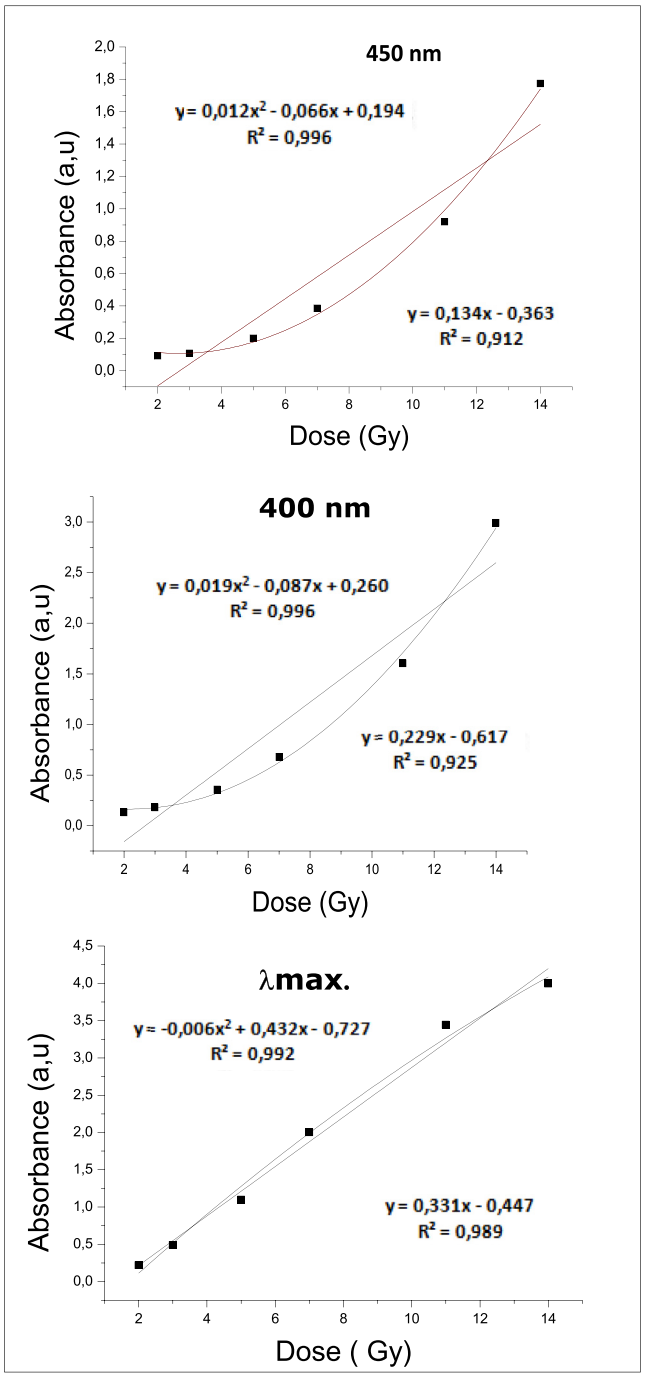

Fig. 8. UV–Visible dose response of polymer gel irradiated by gamma rays at different wavelengths (450, 400 and λ_{max}).

Table 5
Particle size evolution as function of the absorbed dose.

Dose (Gy)	2	3	5	7	11	14
λ_{max} (nm)	313	314	317	320	333	361
D (nm)	288	289	292	294	307	333

optical CT or X-Ray CT which is in good agreement with Watanabe assumption (Watanabe and Warmington, 2017). It has been shown that with an appropriate calibration curve, it is possible for MAGIC to achieved high precision (less than 2%) required for any dosimeter to be considerate as an absolute radiation dosimeter.

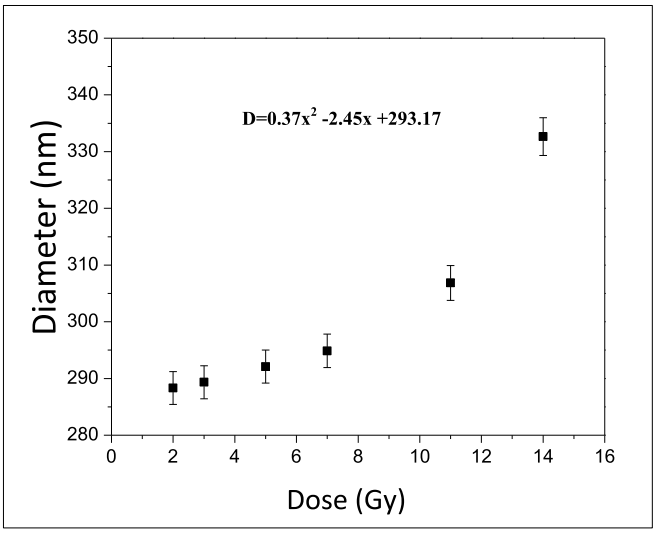

Fig. 9. Evolution of polymerized particles sizes in MAGIC gel as function gamma doses.

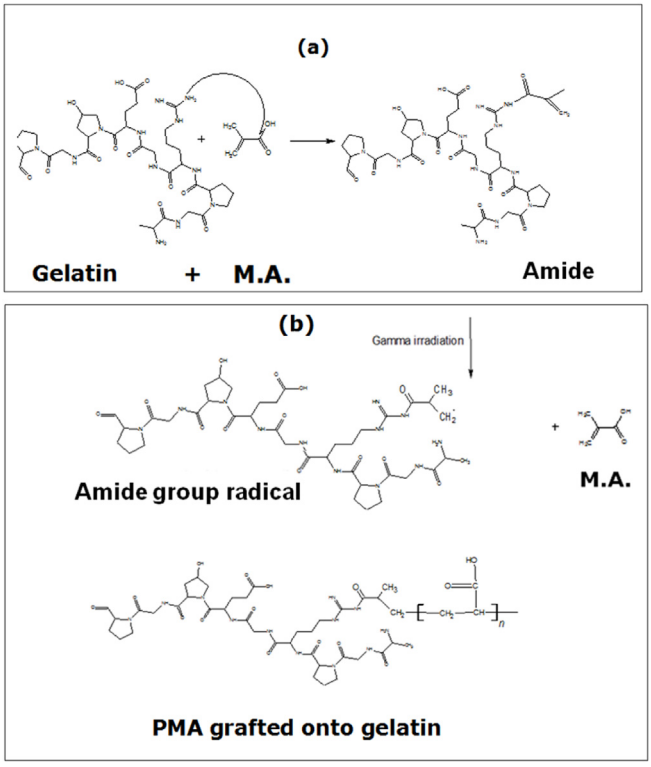

Fig. 10. Proposed mechanistic pathway for M.A. (a) and PMA (b) grafting onto gelatin.

5. Conclusion

The chemical and structural modifications induced by the gamma radiation at different doses in the MAGIC polymer gel were studied using the four selected complementary analyses techniques (FTIR, HPLC, SEM and UV–Visible). The evolution of the polymerization process and the polymerized particles under gamma radiation has been considered to clarify the polymerization mechanism and to improve the dosimetric performance of this system, especially the accuracy of dose measurement and the quality of the calibration relationship using different reading systems specially those based on the attenuation principle such as optical CT or X-Ray CT.

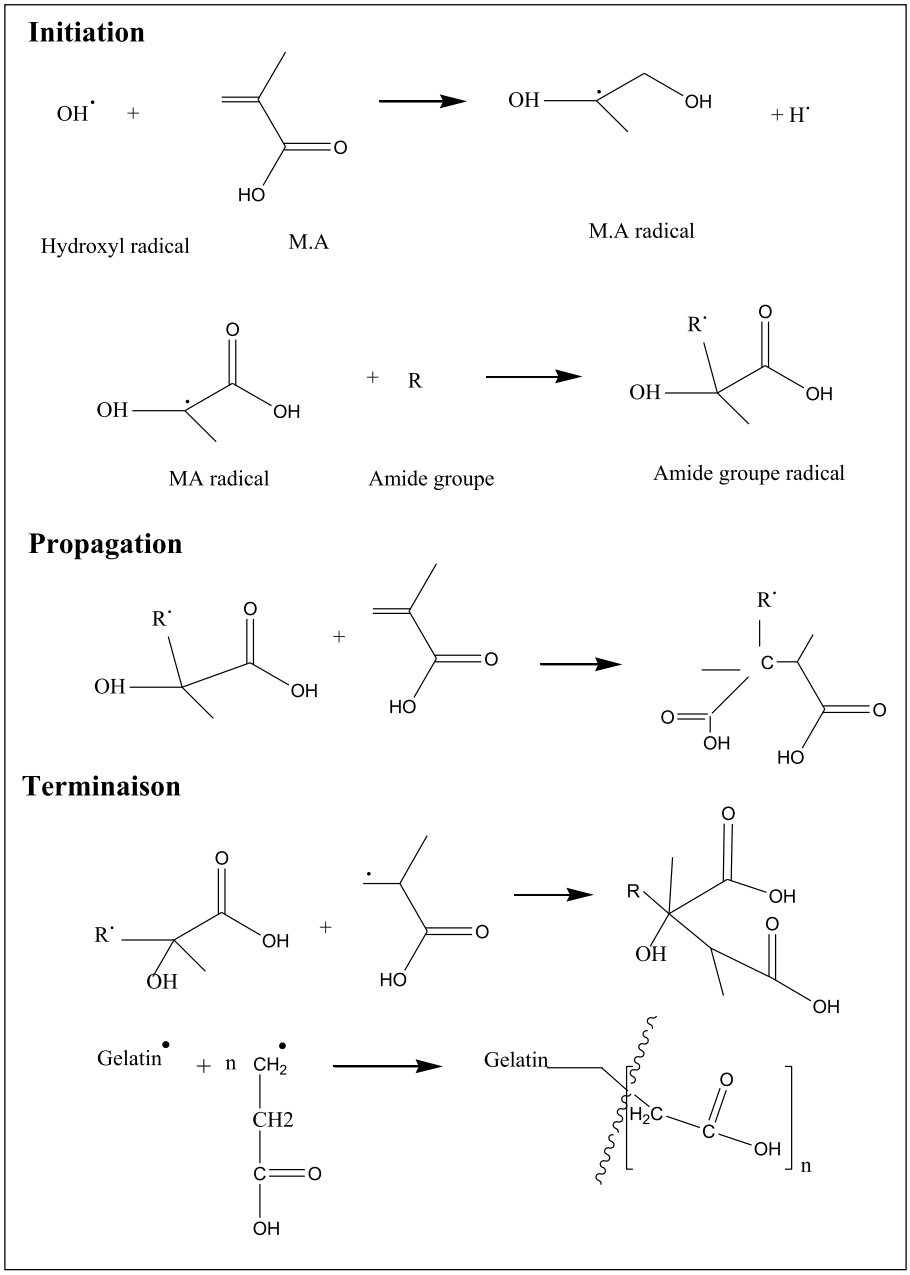

Fig. 11. Proposed mechanism for polymerization M.A in presence of gelatin.

Acknowledgment

The authors wish to gratefully acknowledge Dr Abdelhamid MELLAH the General Director of the Nuclear Research Center of Algiers, Dr Noureddine Gabouze, Director of Research at Semiconductor Technology Research Center for Energetics and Dr Hocine BOUTOUMI Professor at University of Blida for their supporting and interest to this research project.

References

Abdel-Fattah, A.A., Abdel-Hamid, H.M., Radwan, R.M., 2002. Changes in the optical energy gap and ESR spectra of proton irradiated unplasticized PVC copolymer and its possible use in radiation dosimetry. Nucl. Instrum. Methods Phys. Res. B 196, 279 2002.

Audet, C., Schreiner, L., 1999. In: Proceedings of the 1st International Conference on Radiation Therapy Gel Dosimetry, Canadian Organization of Medical Physicists andCanadian College of Physicists in Medicine.

Bäck, S., Olsson, L.E., 2015. In: Proceedings of the 8th International Conference on Radiation Therapy Gel Dosimetry 2014.J. Phys.: Conf. Series, vol. 573.

Baldock, C., DeDeene, Y., 2001. In: Proceedings of the 2st International Conference on Radiation Therapy Gel Dosimetry. Queens l and University of Technology Brisbane, Australia.

Baldock, C., De Deene, Y., 2004. In: Proceedings of the 3rd International Conference on Radiation Therapy Gel Dosimetry 2004: J. Phys. Conf. Series, vol. 3.

Baldock, C., 2006. Historical overview of the development of gel dosimetry: a personal perspective. In: J. Phys. Conf. Series, vol. 56. pp. 14–22.

Baldock, C., De Deene, Y., Doran, S., Ibbott, G., Jirasek, A., Lepage, M., Mc Auley, K.B., Oldham, M., Schreiner, L.J., 2010. Polymer gel dosimeter. Phys. Med. Biol. 55, 1–63.

Baldock, C., 2017. Review of gel dosimetry: a personal reflection. In: J. Phys. Conf. Series, vol. 777. pp. 012029.

Carvalho, R., Grosso, C.R.F., 2008. Properties of chemically modified gelatin films'. Brazilian journal of chemical engineering, Sao Paulo, N 1, pp1322–1331.

De Deene, Y., Hurley, C., Venning, A.J., Vergot, K., Mather, M., Heazly, B.J., Baldock, C., 2002. A basic study of some normoxic polymer gel dosimeters. Phys. Med. Biol. 47, 3441–3463.

De Deene, Y., Vandecasteele, J., 2013. On the reliability of 3D gel dosimeter. J. Phys. Conf. Ser. 444, 12015.

De Deene, Y., Vergote, K., Claeys, C., De Wagter, C., 2006. The fundamental radiation properties of normoxic polymer gel dosimeters: a comparison between a methacrylic

acid based gel and acrylamide based gels. Phys. Med. Biol. 51, 653–673.
Doran, S.J., Koerkamp, K., Bero, M.A., Jenneson, P., Morton, E.J., Gilboy, W.B., 2001. A CCD-based Optical-CT scanner for high-resolution 3D-imaging of radiation dose distribution. Phys. Med. Biol. 12, 3191–3213.
Fong, P.M., Keil, D.C., Does, M.D., Gore, J.C., 2001. Polymer gels for magnetic resonance imaging of radiation dose distributions at normal room atmosphere. Phys. Med. Biol. 46, 3105–3113.
Fontanille, M., Gnanou, Y., 2013. Chimie et physico-chimie des polymères, third ed. Dunod, Paris, France.
Frisch, M.J., Trucks, G.W., Schlegel, H.B., Scuseria, G.E., Robb, M.A., Cheeseman, J.R., Scalmani, G., Barone, V., Mennucci, B., Petersson, G.A., Nakatsuji, H., Caricato, M., Li, X., Hratchian, H.P., Izmaylov, A.F., Bloino, J., Zheng, G., Sonnenberg, J.L., Hada, M., Ehara, M., Toyota, K., Fukuda, R., Hasegawa, J., Ishida, M., Nakajima, T., Honda, Y., Kitao, O., Nakai, H., Vreven, T., Montgomery, J.A., Peralta, J.E., Ogliaro, F., Bearpark, M., Heyd, J.J., Brothers, E., Kudin, K.N., Staroverov, V.N., Kobayashi, R., Normand, J., Raghavachari, K., Rendell, A., Burant, J.C., Iyengar, S.S., Tomasi, J., Cossi, M., Rega, N., Millam, J.M., Klene, M., Knox, J.E., Cross, J.B., Bakken, V., Adamo, C., Jaramillo, J., Gomperts, R., Stratmann, R.E., Yazyev, O., Austin, A.J., Cammi, R., Pomelli, C., Ochterski, J.W., Martin, R.L., Morokuma, K., Zakrzewski, V.G., Voth, G.A., Salvador, P., Dannenberg, J.J., Dapprich, S., Daniels, A.D., Farkas, O., Foresman, J.B., Ortiz, J.V., Cioslowski, J., Fox, D.J., 2009. Gaussian 09, Revision E.01. Gaussian Inc, Wallingford.
Hayashi, S.I., Yoshioka, M., Usui, S., Haneda, K., Tominaga, T., 2010. The role of gelatin in a methacrylic acid based gel dosimeter. Radiat. Phys. Chem. 79, 803–808.
Heather, W.M., Gore, J.C., 2006. Measurement of particle size in polymer gel dosimeters using spectrophotometry. In: J. Phys. Conf. Series, pp. 56160–56163.
Johnston, H., Hilts, M., Carrick, J., Jirasek, A., 2012. An X-ray CT polymer gel dosimetry prototype: gel characterization and clinical application. Phys. Med. Biol. 57, 3155–3165.
Jirasek, A., Hilts, M., 2009. An overview of polymer gel dosimetry using X-ray CT. J. Phys. Conf. Series. 164, 012038.
Jirasek, A., Hilts, M., 2014. Dose calibration optimization and error propagation in polymer gel dosimeter. Phys. Med. Biol. 59, 597–614.
Lepage, M., 2006. Proceedings of the 4th International Conference on Radiation Therapy Gel Dosimetry. J. Phys. Conf. Series 56.
Luci, J.J., Whitney, H.M., Gore, J.C., 2007. Optimization of MAGIC gel formulation for three-dimensional radiation therapy dosimetry. Phys. Med. Biol. 52, 241–248.
Maris, T.G., Pappas, E., 2009. Proceedings of the 5th International Conference on Radiation Therapy Gel Dosimetry 2008. J. Phys. Conf. Series 164.
Oldham, M., Newton, J., 2010. Proceedings of the 6thInternational Conference on Radiation Therapy Gel Dosimetry 2010. J. Phys.: Conf. Series. 250.
RamachandraxG, N., Chandrasekharan, R., 1968. Interchain hydrogen bonds via bound water molecules in the collagen triple helix. Biopolymers 6, 1649–1658.
Samuel, E.J.J., Sathiyaraj, P., Titus, D., Kumar, D.S., 2015. Particle size analysis of PAGAT gel dosimeter. J. Phys. Conf. Ser. 573, 012064.
Schreiner, L.J., 2015. True 3D chemical dosimetry (gels, plastics): development and clinical role. J. Phys. Conf. Ser. 573, 012003.
Schreiner, L.J., 2017. Reviewing three dimensional dosimetry : basics and utilization as presented over 17 Years of DosGel and IC3Ddose. 9th International Conference on 3D Radiation Dosimetry. J. Phys. Conf. Ser. 847.
Siddhartha, S., Devarya, K., Raghuvanshi, S.K., Krishna, J.B.M., Wahab, M.A., 2012. Effect of gamma radiation on the structural and optical proprieties of Polyethylene Terephthalate Polymer (PET). Radiat. Phys. Chem. 81 (4), 458.
Silverstein, R.M., Webster, F.X., Kiemle, D.J., 2015. Spectrometric Identification of Organic Compounds, seventh ed. John wiley and sons, Inc., New York.
Stuart, B.H., 2004. Infrared Spectroscopy: Fundamentals and Applications, Edition. John wiley and sons, New York.
Thwaites, D., Baldock, C., 2013. Proceedings of the 7th international conference on radiation therapy gel dosimetry 2012. J. Phys. Conf. Ser. 444.
Venning, A.J., Nitschke, K.N., Baldock, C., 2004. Radiological properties of normoxic polymer gel dosimeters. Med. Phys. 32, 1047–1053.
Watanabe, Y., Akimitsu, T., Hirokawa, Y., Mooij, R.B., Perera, G.M., 2005. Evaluation of dose delivery accuracy of Gamma Knife by polymer gel dosimetry. J. Appl. Clin. Med. Phys. 6, 133–142.
Watanabe, Y., Kubo, H.A., 2011. Variable echo-number method for estimating R2 in MRI-based polymer gel dosimetry. Med. Phys. 38, 975–982.
Watanabe, Y., Warmington, L., 2017. Three-dimensional radiation dosimetry using polymer gel and solid radiochromic polymer: from basics to clinical applications. World J. Radiol. 9, 112–125.
Webb, S., 2001. Intensity Modulated Radiation Therapy. Series in Medical Physics. Institute of Cancer Research and Royal Marsden.NHS Trust, Sutton, Surrey, UK.
Wickramasinghe, N.C., 1973. Light Scattering Functions for Small Particles, Edition. John Wiley and Son, Inc., New York.
Wüstneck, R., Wetze, F.R., Buder, E., Hermel, H., 1988. The modification of the triple helical structure of gelatin in aqueous solution. The influence of anionic surfactants, pH-value, and temperature. Colloid Polym. Sci. 266, 1061–1067.